

# HIGHER ORDER RADIATIVE CORRECTIONS TO $Z^0$ AND SSC PHYSICS: YFS MONTE CARLO APPROACH<sup>\*,\*\*</sup>

B.F.L. WARD, D. DELANEY, S. JADACH†

CH. SHIO, G. SIOPSIS, M. SKRZYPEK

Department of Physics and Astronomy, The University of Tennessee  
Knoxville, TN 37996-1200, USA

E. RICHTER-WĄS

Institute of Computing Science, Jagellonian University  
Nawojki 11, 30-072 Cracow, Poland.

Z. WĄS†

TH Division, CERN, Geneva 23, Switzerland

AND

S.A. YOST

Department of Physics and Astronomy, The University of Tennessee  
Knoxville, TN 37996-1200, USA

*(Received October 14, 1993)*

We present the recent developments and applications in the Yennie-Frautschi-Suura (YFS) Monte approach to higher order radiative corrections to the  $SU(2)_L \times U_1 \times SU(3)^c$  model of elementary particle interactions. We focus on the high precision  $Z^0$  physics and on recent results relevant to the physics issues for the SSC/LHC type colliding beam device. In both areas of investigation, we conclude that the YFS Monte Carlo approach permits a complete assessment of the role of the higher order radiative effects in the comparison between theory and experiment at the required level of precision.

PACS numbers: 13.40. Ks, 13.10. +q, 12.10. -g, 14.80. Gt

---

\* Presented at the XXXIII Cracow School of Theoretical Physics, Zakopane, Poland, June 1-11, 1993.

\*\* Research supported in part by the US DoE, grant DE-FG05-91ER40627 and contract DE-AC03-76SF00515, by the Texas National Research Laboratory Commission grants RCFY9201 and RCFY93-347 and by the Polish Government grants KBN20389101 and 223729102.

† Permanent address: Institute of Nuclear Physics, Kawory 26a, 30-055 Cracow, Poland.

## 1. Introduction

In Refs [1], two of us (S.J. and B.F.L.W.) introduced the systematic simulation of higher order radiative corrections by Monte Carlo methods which realize the rigorous Yennie–Frautschi–Suura (YFS) [2] cancellation of infrared divergences to all orders in  $\alpha$ . The resulting approach to higher order radiative corrections, which we refer to as the YFS Monte Carlo approach, yields event generators which then simulate the physics processes under study to a well defined precision which can be systematically improved by working to higher and higher order in the respective YFS expansion as it is presented in [2], for example. In particular, the original implementation was in context of high precision  $Z^0$  physics at LEP/SLC. More recently, we have extended [3] the YFS Monte Carlo approach to physics processes of interest to the SSC/LHC type devices. In what follows, we present the current status of the YFS Monte Carlo approach to higher order radiative corrections relative to the respective  $Z^0$  and SSC/LHC physics applications.

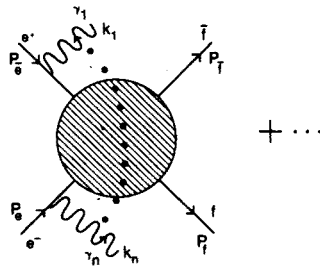


Fig. 1. The process  $e^+e^- \rightarrow \bar{f}f + n(\gamma)$ . Here, the 4-momentum of  $A$  is  $P_A$ ,  $A = e, \bar{e}, f, \bar{f}$ , where  $f$  is a fundamental  $SU_{2L} \times U_1 \times SU(3)^c$  fermion. The 4-momentum of photon  $\gamma_i$  is  $k_i$ ,  $i = 1, \dots, n$ .

More specifically, in Refs [1], two of us (S.J. and B.F.L.W.) introduced the YFS Monte Carlo approach to high precision  $Z^0$  physics for the basic processes  $e^+e^- \rightarrow \bar{f}f + n(\gamma)$ , where  $f$  is a fundamental fermion in the standard  $SU_{2L} \times U_1 \times SU(3)^c$  model [4], as we illustrate in Fig. 1. The cases where  $f$  is and is not the electron resulted in two different realizations of our YFS Monte Carlo methods [1], one *via* the event generator YFS2 [5] which treats the latter case and one *via* the event generator BHLUMI1.xx [6], which treats the former case. We recall that, in the high precision  $Z^0$  physics, the case where  $f = e$  in Fig. 1 has some special significance; for, in that case, at low angles, the respective cross section is used to monitor the LEP/SLC luminosity. Since this luminosity enters into all cross sections at LEP/SLC, the radiative corrections to it are extremely important. For this reason, the pure initial state  $n(\gamma)$  event generator YFS2 was supplemented

by an entirely new event generator, BHLUMI1.xx, which treats initial, final and initial-final interference  $n(\gamma)$  radiation *via* our rigorous YFS Monte Carlo methods. We emphasize that in the LEP/SLC luminosity process, there is no dominant narrow resonance effect to suppress initial-final interference effects and that the highly restrictive phase space of the luminosity acceptance means that even final state radiative effects are important at the desired level of precision. For reference, we note that the original precision of the pure initial state  $n(\gamma)$  event generator YFS2 was  $\leq 0.1\%$  whereas the original precision of BHLUMI1.xx for the LEP/SLC luminosity process was  $1\%$ . As we explain in what follows, recently we have realized  $0.25\%$  precision on the pure QED corrections to the LEP/SLC luminosity process in version 2.01 of BHLUMI [7]. The advent of a new generation of luminosity monitors at LEP [8] has enabled the experimental precision on  $\sigma_L$ , the luminosity cross section, to reach  $0.19\%$  in the ALEPH Collaboration, for example. Accordingly, we comment below on the impending next level of precision which we expect to reach with version 4.xx of BHLUMI.

The fundamental basis of our approach to higher order radiative corrections is then the two key results of YFS in Ref. [2]. Referring to Fig. 1, YFS have shown that the virtual infrared divergences associated with the amplitude  $\mathcal{M}^{(n)}$  depicted therein may be represented as

$$\mathcal{M}^{(n)} = e^{-\alpha B_{\text{YFS}}} \sum_j m_j^{(n)}, \quad (1)$$

and that the real infrared divergences attendant to the cross section associated with the process depicted in this same figure are represented by

$$|\mathcal{M}^{(n)}|^2 = e^{-2\alpha \text{Re} B_{\text{YFS}}} [\tilde{S}_{\text{YFS}}(k_1) \dots \tilde{S}_{\text{YFS}}(k_n) \bar{\beta}_0 + \dots + \bar{\beta}_n(k_1, \dots, k_n)], \quad (2)$$

where the virtual infrared function  $B_{\text{YFS}}$  and the real infrared emission function  $\tilde{S}_{\text{YFS}}$  are both well known [1, 2] explicitly from

$$B_{\text{YFS}} = \frac{-i}{8\pi^3} \int \frac{d^4 k}{(k^2 - \lambda^2 + i\varepsilon)} \left( - \left[ \frac{-2P_e - k}{k^2 + 2kP_e + i\varepsilon} + \frac{-2P_{\bar{e}} + k}{k^2 - 2kP_{\bar{e}} + i\varepsilon} \right]^2 + \dots \right) \quad (3)$$

and

$$\tilde{S}_{\text{YFS}}(k) = \frac{-\alpha}{4\pi^2} \int_{k \leq K_{\text{max}}} \frac{d^3 k}{(k^2 + \lambda^2)^{1/2}} \left( \left( \frac{P_{\bar{e}}}{P_{\bar{e}} k} - \frac{P_e}{P_e k} \right)^2 + \dots \right), \quad (4)$$

where  $\lambda$  is our infrared regulator mass and  $K_{\text{max}}$  is our soft photon energy resolution parameter — it can correspond to a detector resolution parameter

for such soft photons for example. We cannot emphasize too much that no physical cross section can depend on  $K_{\max}$ . The important facts are that  $m_j^{(n)}$  have no virtual infrared divergences to all orders in  $\alpha$  and that the fundamental hard photon residuals  $\bar{\beta}_n$  have neither virtual nor real infrared divergences to all orders in  $\alpha$  [2]. The immediate consequence is that the cross section associated with the process in Fig. 1 can be represented as [2]

$$\sigma_{\text{YFS}} = e^{2\alpha \text{Re} B_{\text{YFS}} + 2\alpha \bar{B}_{\text{YFS}}} \sum_{n=0}^{\infty} \int \prod_{j=1}^n \frac{d^3 k_j}{k_j^0} \int \frac{d^4 y}{(2\pi)^4} \times e^{iy(P_e + P_e - \sum_j k_j - P_f - P_f) + D_{\text{YFS}}} \bar{\beta}_n(k_1, \dots, k_n) \frac{d^3 P_f}{P_f^0} \frac{d^3 P_{\bar{f}}}{P_{\bar{f}}^0}, \quad (5)$$

where we have defined

$$2\alpha \bar{B}_{\text{YFS}} = \int_{k \leq K_{\max}} \frac{d^3 k}{k} \bar{S}_{\text{YFS}}(k) \quad (6)$$

and

$$D_{\text{YFS}} = \int \frac{d^3 k}{k} \bar{S}(k) \left( e^{-iyk} - \theta(K_{\max} - k) \right). \quad (7)$$

We emphasize that (5) is independent of the parameter  $K_{\max}$ . It is the formula (5) that has been realized *via* Monte Carlo methods in Ref. [1] for the first time, wherein the result in [9] was used in a fundamental way. This realization then gave the first ever multiple photon amplitude based event generators in which the cancellation of infrared singularities is effected to all orders in  $\alpha$ .

In particular, the way to high precision  $Z^0$  physics was greatly facilitated by our YFS Monte Carlo based approach to higher order radiative corrections: (a) the physical 4-vectors of the  $n(\gamma)$  system in Fig. 1 were available on an event-by-event basis from the generator; (b) arbitrary detector cuts can be easily accommodated in the generator by simple rejection methods. Hence, the results in Refs [1] corresponded to the first ever realistic high precision  $n(\gamma)$  radiative corrections for  $Z^0$  physics.

What we wish to do in this discussion is to present the current perspective on the YFS Monte Carlo approach to higher order radiative corrections to  $SU(2)_L \times U_1 \times SU(3)^c$  Standard Model processes. We focus on high precision  $Z^0$  physics and on precision SSC/LHC physics. In the former area, we address the current status and outlook for our YFS Monte Carlo realization of the processes  $e^+e^- \rightarrow f\bar{f} + n(\gamma)$ ,  $f \neq e$ , and  $e^+e^- \rightarrow e^+e^- + n(\gamma)$ , ( $\sigma_L$  at LEP/SLC), whereas in the latter area we discuss the current status and

outlook for our extension of our YFS Monte Carlo methods to the realization of the processes  $q + \bar{q}' \rightarrow q'' + \bar{q}''' + n(\gamma)$ ,  $p + p \rightarrow q + \bar{q}' + n(\gamma) + X$  and  $q + \bar{q}' \rightarrow q'' + \bar{q}''' + n(G)$ , where  $G$  is a QCD gluon and  $\bar{q}^{(-) [i, n, m]}$  are (anti-)quarks. The high precision  $Z^0$  physics is presented in the next section; the precision SSC/LHC physics is presented in Section 3. Section 4 contains some summary remarks.

## 2. High precision $Z^0$ physics

In this section, we present the current status and outlook for our YFS Monte Carlo realization of the higher order radiative corrections to the basic processes relevant to high precision  $Z^0$  physics. We begin with the process  $e^+e^- \rightarrow f + \bar{f} + n(\gamma)$ , where  $f \neq e$ .

The practical implementation of the YFS2 event generator for the LEP/SLC physics of the processes  $e^+e^- \rightarrow f\bar{f} + n(\gamma)$ ,  $f \neq e$ , has been effected via the program KORALZ3.8 [10], wherein three of us (S.J., B.F.L.W. and Z.W.) have integrated YFS2 with the  $\mathcal{O}(\alpha)$  electroweak radiative correction libraries of Bardin *et al.* [11] and of Hollik [12], where in the case that  $f = \tau$  the tau decay module Tauola [13] is also included. The result is that KORALZ3.8 is the unique multiple photon event generator with the YFS  $n(\gamma)$  initial state radiation from YFS2,  $1\gamma$  final state radiation and  $\mathcal{O}(\alpha)$  pure weak corrections. The respective QED corrections are then accurate to  $\leq 0.1\%$ . The typical set of Feynman graphs treated by KORALZ3.8 is illustrated in Fig. 2; it is now in wide use at LEP/SLC.

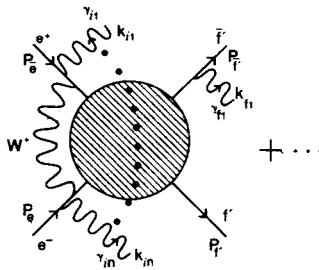


Fig. 2. Multiple photon radiation from the initial state and single photon radiation from the final state in the presence of pure weak one-loop corrections in  $e\bar{e} \rightarrow f\bar{f} + (n+1)\gamma$ , with the same kinematical conventions as those in Fig. 1.

For example, consider the case when  $f = \tau$  in Fig. 2, so that we have the process  $e^+e^- \rightarrow \tau\bar{\tau} + n(\gamma)$ . There is available as a LEP observable the fundamental  $\tau$  polarization asymmetry  $A_{\text{pol}}^\tau$ , whose Born level expected

value is

$$A_{\text{pol}}^{\tau} = \frac{2a_{\tau}v_{\tau}}{a_{\tau}^2 + v_{\tau}^2} \quad (8)$$

when  $a_{\tau}$  and  $v_{\tau}$  are the respective axial-vector and vector couplings of the  $\tau$  to the  $Z^0$ . The initial state radiation shifts  $A_{\text{pol}}^{\tau}$  by 1.7% at the  $Z^0$  peak and, using KORALZ3.8, we control this shift to  $< 0.07\%$ . The measured value of  $A_{\text{pol}}^{\tau}$  is an important part of the high precision  $Z^0$  physics tests of the Standard Model and KORALZ3.8, by providing realistic event simulations of the respective  $Z^0$  production and decay processes, plays an essential role in the respective data analysis and interpretation [14].

Recently we have developed two new directions in our YFS2-based research. We will now describe these two directions in turn.

First, two of us (S.J. and B.F.L.W.) have extended the YFS2 program to include multiple final state radiative effects in our YFS Monte Carlo framework, as illustrated in Fig. 3. The resulting Monte Carlo event generator is the program YFS3 [15] and describes the realistic event-by-event simulation of both initial state and final state  $n(\gamma)$  radiative effects in the processes  $e^+e^- \rightarrow f\bar{f} + n(\gamma)$ ,  $f \neq e$ . YFS3 has already found wide use at LEP.

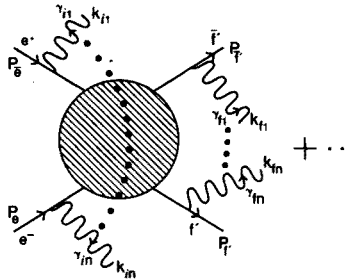


Fig. 3. Multiple photon radiation from the initial state and the final state (pure weak effects may be present in the underlying interactions) in  $e\bar{e} \rightarrow f'\bar{f}' + (n+1)\gamma$ , with the same kinematical conventions as those in Fig. 1.

To illustrate this use, consider the recent excitement generated by the L3 observations [16] of the processes  $e^+e^- \rightarrow \ell\bar{\ell} + \gamma\gamma$ , where  $\ell$  is a charged lepton and one focuses on large values of the  $M_{\gamma\gamma}$ , the  $\gamma\gamma$  invariant mass. The comparison of the L3 data with our absolutely normalized YFS3 prediction for the  $M_{\gamma\gamma}$  distribution is shown in Fig. 6 of Ref. [16]. At the time of this plot, the clustering of events near  $M_{\gamma\gamma} = 60$  GeV represented a 0.1% fluctuation above the YFS3 prediction when due account is taken of accuracy of the YFS3 result in the respective region of  $\gamma\gamma$  phase space. Recently, all LEP collaborations have searched for similar events as those found by

L3 and have used YFS3 in assessing their findings [17]. The conclusions are currently that the significance of the clustering near  $M_{\gamma\gamma} = 60$  GeV is that of a  $\sim 2\%$  fluctuation and that more data are needed to definitively clarify the situation.

Secondly, we note that three of us (S.J., B.F.L.W. and Z.W.) are developing version 4.0 of KORALZ [18] which combines the program YFS3 with KORALZ3.8 so that one has YFS Monte Carlo simulation of both initial and final state  $n(\gamma)$  radiative effects in the presence of the pure weak  $\mathcal{O}(\alpha)$  radiative corrections libraries of Bardin *et al.* [11] and of Hollik [12] as well as access to the  $\tau$  decay library Tauola [13]. This program is in its testing stages and will be available for public distribution in the near future [18]. We expect KORALZ4.0 to have even wider use than version 3.8 at LEP/SLC in view of the recent interest in final state radiation at LEP [19].

Turning next to the important LEP/SLC luminosity process  $e^+e^- \rightarrow e^+e^- + n(\gamma)$ , we note that four of us (S.J., E.R.-Was, B.F.L.W. and Z.W.) have recently published [7] and distributed version 2.01 of the YFS Monte Carlo program BHLUMI. The main result of this new version of BHLUMI is that the LEP/SLC luminosity process is simulated to 0.25% precision insofar as the QED radiative effects are concerned. The contribution from the  $\gamma - Z^0$  interference effect is treated as the lowest order and recent work by Beenakker and Pietrzyk [20] gives an additional effect of  $\approx 0.2\%$  for the  $\mathcal{O}(\alpha)$  correction to this interference at  $s = M_{Z^0}^2$ , for example. In our original error analysis for BHLUMI, which is given in Table 2 of the second paper in Ref. [7], we estimated the size of this correction to be bounded by 0.03%, somewhat lower than the result in Ref. [20]. Accordingly, until we incorporate the correction into BHLUMI, one may conservatively add an additional error of 0.2% in quadrature with the pure QED error of 0.25% quoted in Ref. [7] to get a total precision of 0.3% for the LEP/SLC luminosity cross section as calculated by BHLUMI2.01 for the typical LEP/SLC scattering angle acceptance of  $\approx 3^\circ - 6^\circ$ , for example, at  $s = M_{Z^0}^2$ . This is the highest precision ever achieved in a calculation of low angle Bhabha scattering at high cms energies. BHLUMI is in wide use at LEP/SLC; it opens the way to 0.1% tests of the Standard Model in  $Z^0$  physics.

Indeed for the 1991 LEP data, the 0.3% accuracy on BHLUMI2.01 was quite adequate; for, the smallest experimental error on the respective luminosity cross section was that of the ALEPH Collaboration and was 0.45% [21], so that the error on BHLUMI's result was still small compared to that of the experimental results. For the 1992 data, the situation has been changed by the advent of a new class of luminosity monitoring devices at LEP whose aim is to reduce the experimental error to the 0.1% or below regime — this is what one really needs for 0.1% precision  $Z^0$  physics. Indeed, already the ALEPH Collaboration [22] has reported that its new luminos-

ity monitor, with an acceptance of  $1.4^0$ - $3.3^0$ , has allowed it to achieve the experimental systematic error of 0.152% for its luminosity cross section in the 1992 data. This means that the precision of BHLUMI needs to be improved to the 0.05% regime in the near future so that the theoretical error on the luminosity cross section will not prevent 0.1% comparison between the Standard Model predictions and the experimental observations in high precision  $Z^0$  physics. Accordingly, we are now in the process of making the improvement in BHLUMI [23].

Specifically, referring to Table 2 in the second paper in Ref. [7], we see that the higher order corrections to the bremsstrahlung process are a large part of the error in the BHLUMI2.01 cross section. Recently, three of us (S.J., B.F.L.W. and S.Y.) have computed [24] the exact result for the two photon bremsstrahlung process  $e^+e^- \rightarrow e^+e^- + 2\gamma$ . This result allows us to remove the error due to the missing bremsstrahlung corrections as quoted in Table 2 of the second paper in Ref. [7]. Similarly, the missing corrections for the pairs production listed in the latter table (hereafter referred to as Table 2) have recently been computed [25] by three of us (S.J., M.S. and B.F.L.W.) and are currently being implemented at the level of a Monte Carlo. This then allows us to remove the errors due to soft pairs in BHLUMI2.01. The error listed for the  $Z^0$  exchange effect in Table 2 has been discussed above; the effect is computed in Ref. [20] in detail and we are currently checking [26] the respective result. Hence, this will allow us to remove the error due to the  $Z^0$  exchange effect from BHLUMI2.01.

Finally, we note that the smaller acceptance of the new luminosity monitors compared to the older ones will reduce the error due to hadronic vacuum polarization in Table 2 to below 0.05% [22]. This means that, in view of the improvements just described for the other errors in Table 2, the total precision in the respective impending new version of BHLUMI, which we will call version 4.00, will be indeed  $\sim 0.05\%$ , as desired. Implied in this latter statement is the ability to check both the physical and technical precision of the respective implementation of the hard photon residuals  $\beta_i$ ,  $i = 0, 1, 2$  to the  $< 0.02\%$  precision level. Here the primary physical effect needed which is not readily available in the literature is the exact  $\mathcal{O}(\alpha)$  correction to the single bremsstrahlung process [27], where the original work in [28] is not sufficient because it is not completely differential, for example. Recently, a sufficient accurate version of the required result has appeared [29]; our exact expression should be available soon as well. (We need to mention that very useful work by the authors in Ref. [30] on the  $\mathcal{O}(\alpha^2)$  virtual corrections to low angle Bhabha scattering is now available for checking our work on the analogous corrections to  $\beta_0$ . The work in Ref. [29] is also useful in this regard.)

We conclude that high precision  $Z^0$  physics at the  $\sim 0.1\%$  level is near



and that our YFS Monte Carlo methods have played and will continue to play a significant role in that physics. We turn now to the extension of these methods to LHC/SSC processes. This is the subject of the next section.

### 3. Precision SSC/LHC physics

In this section we discuss the extension of our YFS Monte Carlo methods to precision SSC physics issues. We shall discuss both multiple photon effects and multiple gluon effects in this context. We begin with multiple photon effects in the processes  $q + \bar{q}' \rightarrow q'' + \bar{q}''' + n(\gamma)$  and  $p + p \rightarrow q + \bar{q}' + X$ .

Specifically, in [3] five of us (D.D., S.J., Ch.S., G.S. and B.F.L.W.) have effected the extension of the YFS2 Monte Carlo calculation in [2] to the basic fermion-(anti)-fermion scattering processes at SSC/LHC energies in the SDC/GEM type acceptances. This extension of YFS2, which we denote by SSCYFS2, then allows the event-by-event realization of multiple photon radiative effects in the SSC/LHC environment at the level of quarks, where the cancellation of the respective infrared divergences is effected to all orders in  $\alpha$ . The details of the extension may be found in [3]. Here, we emphasize that, due to the lack of a prominent resonance in the underlying QCD processes, the background MC [2] in SSCYFS2 had to made significantly different from that in YFS2 in order to maintain a reasonable rejection efficiency. In addition, the numerical work in SSCYFS2 had to be improved over that in YFS2 in order to control machine rounding errors. We want to emphasize that the fundamental running quark masses play the same role in SSCYFS2 that the electron mass plays in YFS2: they determine the probability to radiate in the initial state of the underlying QCD hard processes *via* the usual formula

$$P(k > \bar{k}_0) = \frac{2\alpha Q_f^2}{\pi} \left( \ln \frac{\hat{s}}{m_f^2} - 1 \right) \ln \frac{\sqrt{\hat{s}}}{2\bar{k}_0}, \quad (9)$$

where  $Q_f$  and  $m_f$  are the electric charge and rest mass of the fermion  $f$  when the electric charge is measured in units of the positron charge. It is in this way that SSCYFS2 controls the absolute normalization of multiple photon radiative effects at the quark level in SSC/LHC processes.

We illustrate the capabilities of SSCYFS2 in Fig. 4 and 5 for the processes  $u + u \rightarrow uu + n(\gamma)$  at  $\sqrt{s} = 40$  TeV (entirely similar results hold for  $\sqrt{s} = 6.7$  TeV [3]). What we show in Fig. 4 is the photon multiplicity for the SDC and GEM acceptance  $|\eta| \leq 2.8$  for photon energies  $E_\gamma > 20$  MeV in the cms system. We see that the average number of such photons per event is

$$\langle n_\gamma \rangle = 0.85 \pm 0.92. \quad (10)$$

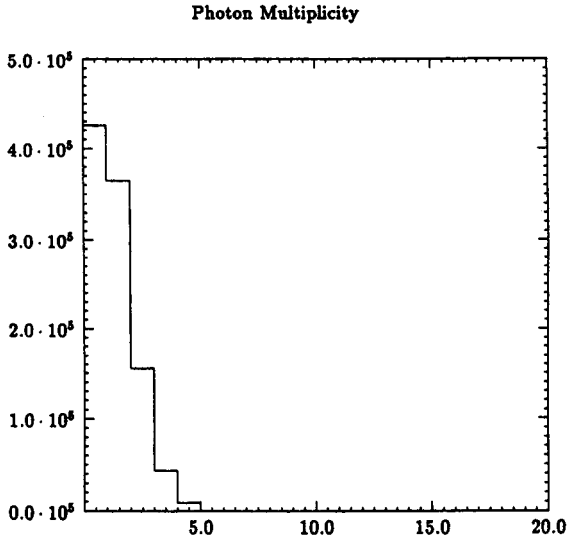


Fig. 4. Photon multiplicity in  $u + u \rightarrow u + u + n(\gamma)$  at  $\sqrt{s} = 40$  TeV. Similar results hold for  $\sqrt{s} = 6.7$  TeV [3].

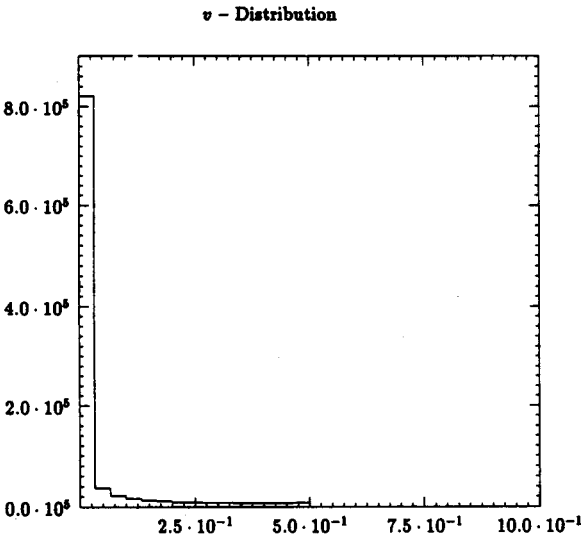


Fig. 5.  $v$ -distribution for  $u + u \rightarrow u + u + n(\gamma)$  at  $\sqrt{s} = 40$  TeV. Similar results hold for  $\sqrt{s} = 6.7$  TeV [3].

Similarly, in Fig. 5 we show the  $v \equiv (s - s')/s$  distribution for the same SDC/GEM acceptance. The respective average value is

$$\langle v \rangle = 0.05 \pm 0.09. \quad (11)$$

Thus in both figures, we see that these  $n(\gamma)$  effects must be taken into account for precise SSC/LHC physics simulations.

The discussion of  $n(\gamma)$  effects at the quark level allows a natural extension of such effects at the hadron level. We can effect the corresponding extension either in the usual parton model or in the amplitude-based method of Lepage and Brodsky [31]. Here we discuss the former approach; the latter approach will be taken-up elsewhere [32]. Specifically, in Ref. [3], we have used the standard parton model formula for the process  $p + p \rightarrow q + \bar{q}' + X$  so that respective cross section is represented as

$$\sigma = \int \sum_{j,j'} D_j(x_1) D_{j'}(x_2) \sigma_{\text{YFS}}(x_1 x_2 s) dx_1 dx_2, \quad (12)$$

where  $D_j$  are the usual parton distribution functions and  $x_i$  are the respective light cone momentum fractions of partons  $j$  and  $j'$ . Using SSCYFS2 for the cross section  $\sigma_{\text{YFS}}$  in (12), we have realized the RHS (right-hand side) of the last equation *via* Monte Carlo methods in the program SSCYFSP [3]. In this way, we get the results in Figs 6 and 7 for the number of radiated photons and that  $v$ -distribution, respectively. We see that the corresponding average values of  $n_\gamma$  and  $v$  are, for  $\sqrt{s} = 40$  TeV,

$$\langle n_\gamma \rangle = 0.133 \pm 0.369 \quad (13)$$

and

$$\langle v \rangle = 0.018 \pm 0.067. \quad (14)$$

Thus, we again conclude that the multi-photon effects must be taken into account for precise SSC/LHC physics simulations, such as those required to assess the discovery prospects for the Higgs particle of intermediate mass *via* the decay  $H \rightarrow \gamma\gamma$ , for example [32].

While the  $n_\gamma$  effects are significant, clearly the dominant radiative effects in SSC/LHC physics are due to gluon radiation. In this latter context, with an eye toward precision SSC/LHC physics, recently we have shown [33] that the YFS theory can be extended to soft gluons in QCD. Specifically, from the graphs in Fig. 8 for the process (the relevant kinematics is summarized in the figure)  $q + \bar{q}' \rightarrow q + \bar{q}' + (G)$ , we follow the prescription of

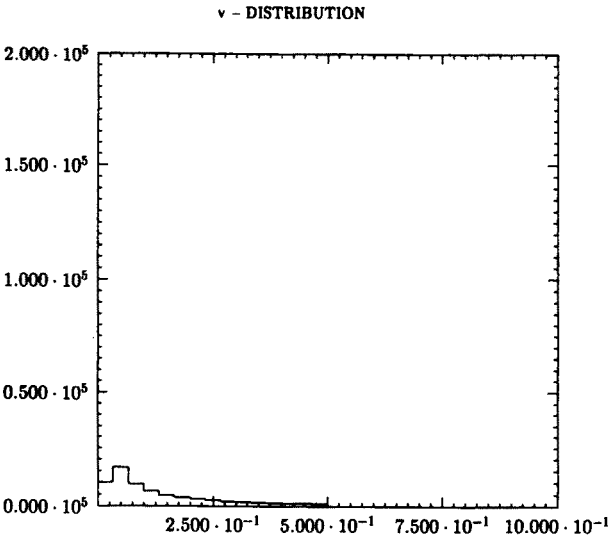


Fig. 6. Photon multiplicity in  $p + p \rightarrow q + \bar{q}' + X + n(\gamma)$  at  $\sqrt{s} = 40$  TeV.

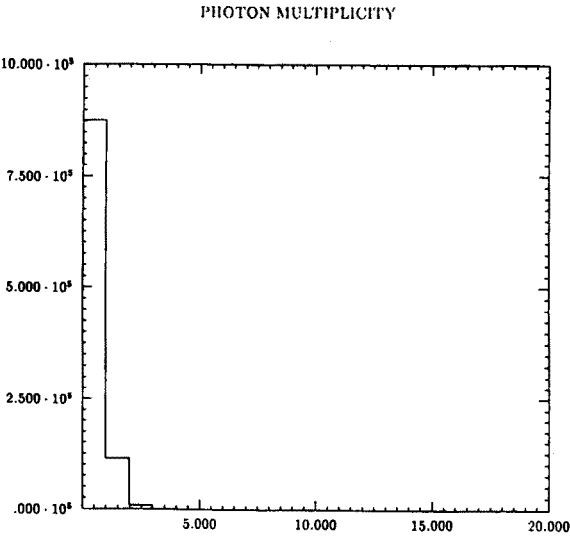


Fig. 7.  $v$ -distribution in  $p + p \rightarrow q + \bar{q}' + X + n(\gamma)$  at  $\sqrt{s} = 40$  TeV.

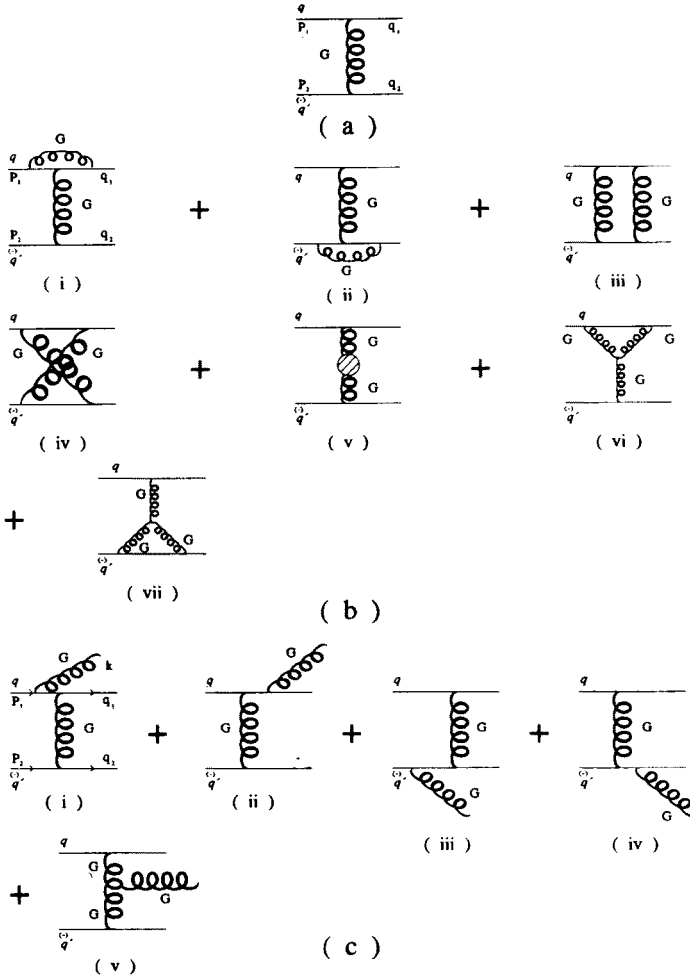


Fig. 8. The process  $q + \bar{q}' \rightarrow q + \bar{q}' + (G)$  to  $O(\alpha_s)$ : (a) Born approximation; (b)  $O(\alpha_s)$  virtual correction; (c)  $C(\alpha_s)$  bremsstrahlung process.

YFS for the QCD analogue of the YFS real and virtual infrared functions  $\tilde{B}_{\text{YFS}}$  and  $B_{\text{YFS}}$ , respectively. We get [33] for QCD the results

$$B_{\text{QCD}} =$$

$$\begin{aligned} & \frac{i}{(8\pi^3)} \int \frac{d^4 k}{(k^2 - m_G^2 + i\epsilon)} \left[ C_F \left( \frac{2p_1 + k}{k^2 + 2k \cdot p_1 + i\epsilon} + \frac{2p_2 - k}{k^2 - 2k \cdot p_2 + i\epsilon} \right)^2 \right. \\ & \left. + \Delta C_s \frac{2(2p_1 + k) \cdot (2p_2 - k)}{(k^2 + 2k \cdot p_1 + i\epsilon)(k^2 - 2k \cdot p_2 + i\epsilon)} \right] \end{aligned}$$

$$\begin{aligned}
& + C_F \left( \frac{2q_1 + k}{k^2 + 2k \cdot q_1 + i\epsilon} + \frac{2q_2 - k}{k^2 - 2k \cdot q_2 + i\epsilon} \right)^2 \\
& + \Delta C_s \frac{2(2q_1 + k) \cdot (2q_2 - k)}{(k^2 + 2k \cdot q_1 + i\epsilon)(k^2 - 2k \cdot q_2 + i\epsilon)} \\
& + C_F \left( \frac{2p_2 + k}{k^2 + 2k \cdot p_2 + i\epsilon} - \frac{2q_2 + k}{k^2 + 2k \cdot q_2 + i\epsilon} \right)^2 \\
& - \Delta C_t \frac{2(2q_2 + k) \cdot (2p_2 + k)}{(k^2 + 2k \cdot q_2 + i\epsilon)(k^2 + 2k \cdot p_2 + i\epsilon)} \\
& + C_F \left( \frac{2p_1 + k}{k^2 + 2k \cdot p_1 + i\epsilon} - \frac{2q_1 + k}{k^2 + 2k \cdot q_1 + i\epsilon} \right)^2 \\
& - \Delta C_t \frac{2(2p_1 + k) \cdot (2q_1 + k)}{(k^2 + 2k \cdot p_1 + i\epsilon)(k^2 + 2k \cdot q_1 + i\epsilon)} \\
& - C_F \left( \frac{2p_1 + k}{k^2 + 2k \cdot p_1 + i\epsilon} - \frac{2q_2 + k}{k^2 + 2k \cdot q_2 + i\epsilon} \right)^2 \\
& + \Delta C_u \frac{2(2p_1 + k) \cdot (2q_2 + k)}{(k^2 + 2k \cdot p_1 + i\epsilon)(k^2 + 2k \cdot q_2 + i\epsilon)} \\
& - C_F \left( \frac{2q_1 + k}{k^2 + 2k \cdot q_1 + i\epsilon} - \frac{2p_2 + k}{k^2 + 2k \cdot p_2 + i\epsilon} \right)^2 \\
& + \Delta C_u \frac{2(2q_1 + k) \cdot (2p_2 + k)}{(k^2 + 2k \cdot q_1 + i\epsilon)(k^2 + 2k \cdot p_2 + i\epsilon)} \Big] \quad (15)
\end{aligned}$$

and

$$2\alpha_s \tilde{B}_{\text{QCD}} = \int \frac{d^3 k}{k_0} \tilde{S}_{\text{QCD}}(k) \quad (16)$$

with

$$\begin{aligned}
\tilde{S}_{\text{QCD}}(k) = & -\frac{\alpha_s}{4\pi^2} \left\{ C_F \left( \frac{p_1}{p_1 \cdot k} - \frac{q_1}{q_1 \cdot k} \right)^2 - \Delta C_t \frac{2p_1 \cdot q_1}{k \cdot p_1 k \cdot q_1} \right. \\
& + C_F \left( \frac{p_2}{p_2 \cdot k} - \frac{q_2}{q_2 \cdot k} \right)^2 - \Delta C_t \frac{2p_2 \cdot q_2}{k \cdot p_2 k \cdot q_2} + C_F \left( \frac{p_1}{p_1 \cdot k} - \frac{p_2}{p_2 \cdot k} \right)^2 \\
& - \Delta C_s \frac{2p_1 \cdot p_2}{k \cdot p_1 k \cdot p_2} + C_F \left( \frac{q_1}{q_1 \cdot k} - \frac{q_2}{q_2 \cdot k} \right)^2 - \Delta C_s \frac{2q_1 \cdot q_2}{k \cdot q_1 k \cdot q_2} \\
& - C_F \left( \frac{q_1}{q_1 \cdot k} - \frac{p_2}{p_2 \cdot k} \right)^2 + \Delta C_u \frac{2q_1 \cdot p_2}{k \cdot q_1 k \cdot p_2} - C_F \left( \frac{q_2}{q_2 \cdot k} - \frac{p_1}{p_1 \cdot k} \right)^2 \\
& \left. + \Delta C_u \frac{2q_2 \cdot p_1}{k \cdot q_2 k \cdot p_1} \right\}, \quad (17)
\end{aligned}$$

where  $C_F = 4/3$  = quadratic Casimir invariant of the quark color representation,  $m_G$  is a standard infrared regulator mass and

$$\begin{aligned}\Delta C_s &= \begin{cases} -1, & \text{qq' incoming} \\ -1/6, & \text{q}\bar{\text{q}}' \text{ incoming} \end{cases}, \quad \Delta C_t = -3/2, \text{ and} \\ \Delta C_u &= \begin{cases} -5/2, & \text{qq' incoming} \\ -5/3, & \text{q}\bar{\text{q}}' \text{ incoming} \end{cases}, \end{aligned} \quad (18)$$

and we always assume an SDC/GEM trigger such that  $|q^2| = |(p_1 - q_1)^2| \gg \Lambda_{\text{QCD}}^2$  and  $|q'^2| = |(p_2 - q_2)^2| \gg \Lambda_{\text{QCD}}^2$ .

The important fact is that graphs (v)–(vii) in Fig. 8b and (v) in Fig. 8c do not contribute to the infrared singularities in the respective cross sections. More important is the fact that

$$\text{SUM}_{\text{IR}}(\text{QCD}) = 2\alpha_s \text{Re} B_{\text{QCD}} + 2\alpha_s \tilde{B}_{\text{QCD}}(K_{\text{max}}) \quad (19)$$

is also infrared finite: for  $m_q = m_{q'} = m$ , for example, we get

$$\text{SUM}_{\text{IR}}(\text{QCD}) = \frac{\alpha_s}{\pi} \sum_{A=\{s,t,u,s',t',u'\}} (-1)^{\rho(A)} (C_F B_{\text{tot}}(A) + \Delta C_A B'_{\text{tot}}(A)), \quad (20)$$

where

$$B_{\text{tot}}(A) = \log \left( \frac{2K_{\text{max}}}{\sqrt{|A|}} \right)^2 \left( \ln \left( \frac{|A|}{m^2} \right) - 1 \right) + \frac{1}{2} \ln \frac{|A|}{m^2} - \frac{\pi^2}{6} + \theta(A) \frac{\pi^2}{2} \quad (21)$$

and

$$\rho(A) = \begin{cases} 0, & A = s, s', t, t' \\ 1, & A = u, u' \end{cases}. \quad (22)$$

(The general expression for (20) with  $m_q \neq m_{q'}$  can be infrared from Refs [1, 2, 34] and [35] and it is in agreement with the infrared cancellations in (20).) Thus, for soft gluons with wavelengths  $\gg 1/\Lambda_{\text{QCD}}$ , we find that we may carry through the methods of YFS to QCD [36]. In concluding that we can carry through the methods of Ref. [2] from (15)–(22), we are using the same exponentiation algebra as that given therein, where the only difference is that, here, each channel of the  $s, t$  and  $u$  channels has a different weight in  $B_{\text{QCD}}$  and  $\tilde{B}_{\text{QCD}}$  which depends on  $C_F$  and  $C_A = 3$ , whereas in QED corresponding weights only depend on the electric charges of the respective interacting fermions. Alternatively, one can use the pioneering results of Berends and Giele in Ref. [37] to conclude that the infrared radiation factorizes in QCD so that our results (15)–(22) can be substituted directly into the YFS exponentiation result. (Here,  $C_A$  is the gluon Casimir invariant.)

Specifically, our exponentiated multiple gluon cross section takes the form

$$d\sigma_{\text{exp}} = e^{\text{SUM}_{\text{IR}}(\text{QCD})} \sum_{n=0}^{\infty} \int \prod_{j=1}^n \frac{d^3 k_j}{k_j} \int \frac{d^4 y}{(2\pi)^4} e^{iy \cdot (p_1 + p_2 - q_1 - q_2 - \Sigma k_j) + D_{\text{QCD}}} \\ * \bar{\beta}_n(k_1, \dots, k_n) \frac{d^3 q_1 d^3 q_2}{q_1^0 q_2^0} \quad (23)$$

and

$$D_{\text{QCD}} = \int \frac{d^3 k}{k} \tilde{S}_{\text{QCD}}(k) \left[ e^{-iy \cdot k} - \theta(K_{\text{max}} - k) \right], \quad (24)$$

$$\bar{\beta}_0 = d\sigma^{(1\text{-loop})} - 2\alpha_s \text{Re} B_{\text{QCD}} d\sigma_B,$$

$$\bar{\beta} = d\sigma^{B1} - \tilde{S}_{\text{QCD}}(k) d\sigma_B, \dots, \quad (25)$$

where  $d\sigma^{(1\text{-loop})}$  is the  $O(\alpha_s)$  cross section for Figs 8a and b [38],  $d\sigma^{B1}$  is the cross section for Fig. 8c [39], and  $d\sigma_B$  is the Born cross section for Fig. 8a. Formulas for the remaining  $\bar{\beta}_n$  can be inferred from Refs [1, 2, 32, 34]; we show only the  $\bar{\beta}_i$  relevant to exact  $O(\alpha_s)$  exponentiation for the sake of pedagogy. Note that the dummy parameter  $K_{\text{max}}$  may correspond to an experimental detector resolution for soft gluon jet energies; we emphasize that (23) is independent of  $K_{\text{max}}$ , in complete analogy with the corresponding circumstance in QED.

The hard gluon residuals  $\bar{\beta}_n$  in (23) can be improved *via* the usual renormalization group methods in complete analogy with the renormalization group improvement of the QED YFS hard photon residuals  $\bar{\beta}_n$  in Ref. [34]. This follows from the fact that QCD, like QED is a renormalizable quantum field theory, which is perturbatively calculable so long as the relevant momentum transfer squared is large compared to  $\Lambda_{\text{QCD}}^2$ . This latter requirement is satisfied for (23), where we have in mind the SDC/GEM acceptances at the SSC for  $\sqrt{s} = 40$  TeV pp collisions. Following the arguments in Ref. [34], we conclude that we get the renormalization group improved version of (23) by making the substitutions in (23) (here we use the standard notation [40] for the running masses  $m_i(\lambda)$  and the scaled external momenta  $\{\lambda \bar{p}_i\}$ )

$$\bar{\beta}_n(\lambda\{\bar{p}_i\}; m_i, \alpha_s) \rightarrow \lambda^{2D_r} \bar{\beta}_n(\{\bar{p}_i\}; m_i(\lambda), \alpha_s(\lambda)) \exp \left[ - \int_1^{\lambda} \frac{d\lambda' 2\gamma_r(\lambda')}{\lambda'} \right], \quad (26)$$



where  $D_\Gamma$  is the respective engineering dimension of the amplitude from which  $\bar{\beta}_n$  is constructed and  $\gamma_\Gamma$  is the anomalous dimension of the amplitude [40]. (We allow that a finite renormalization group transformation may have been used to implement Weinberg's renormalization group operator at a convenient off-shell point and to return our amplitude to the mass shell thereafter.) In this way, we arrive at the renormalization group improved exponentiated multiple gluon theory which is entirely analogous to the renormalization group improved YFS theory in Ref. [34] for QED.

The results (23) and (26) lend themselves to the same kind of Monte Carlo event generator realization as did the theory in Ref. [34]. We have constructed two such event generators from (23) and (26), one of which, SSCBHLG, treats multiple gluon radiation from both initial and final states, and the other of which, SSCYFSG, treats multiple gluon radiation from the initial state only. These two Monte Carlo event generators will be discussed in detail elsewhere [32].

We conclude this section by emphasizing that our multiple gluon Monte Carlo programs SSCYFSG and SSCBHLG have a sound theoretical basis: the way the precision SSC/LHC physics is now open. Indeed, we can report for example the sample preliminary result from SSCBHLG that, for the SDC/GEM type cuts, in the process  $u+u \rightarrow u+u+n(G)$  for  $\sqrt{s} = 40$  TeV, the average number of gluons with energy greater than 3 GeV is  $\langle n_G \rangle \approx 15 - 30$  per event. Clearly, these have to be treated properly to assess SSC/LHC physics reliably.

#### 4. Conclusions and outlook

What we have shown in our discussion is that the high precision  $Z^0$  physics is approaching the 0.1% regime, where we recall that the generic weak loop effect is of size  $\frac{\alpha}{\pi} \approx 0.23\%$ . This means that  $\sim 2 \times 10^7 Z^0$ 's at LEP would be very useful in taking full advantage of this 0.1% regime for testing the Standard Model. We therefore encourage the LEP experimentalists to strive to achieve this level of detected  $Z^0$ 's.

The high precision SSC/LHC physics is now possible for the  $n(\gamma)$  effects, at 0.1% precision, at the parton level using SSCYFS2 [3]. The analogous results for pp scattering are available using SSCYFSP [3] with the usual parton model dependence of the respective precision. We are working on a realization of such results *via* the Lepage-Brodsky approach to hadron-hadron processes which would reduce this latter model dependence of the respective precision [32].

Precision  $n(G)$  SSC/LHC physics, at  $\sim 3\%$  precision at the parton level, is near, where  $G$  denotes QCD gluon. Here the precise extension to the hadron level will involve the Lepage-Brodsky methods as well.

We may, therefore, state that YFS Monte Carlo methods and their extensions to QCD have a broad reach in Standard Model physics. This reach may even take us beyond the latter model.

One of the authors (B.F.L.W.) is grateful to Prof. A. Bialas and the Organizing Committee for giving him the opportunity to participate in the XXXIII Cracow School of Theoretical Physics. The authors have benefited from the kind hospitality of Profs. M. Breidenbach, J. Dorfan and C. Prescott of SLAC, of Prof. J. Ellis of the CERN TH Division, and of Profs. W. Bardeen and F. Gilman of SSCL at various stages of the development of the material presented in the text.

### REFERENCES

- [1] See for example S. Jadach, B.F.L. Ward, *Phys. Rev.* **D38**, 2897 (1988); *Phys. Lett.* **B220**, 611 (1989) and references therein.
- [2] D.R. Yennie, S.C. Frautschi, H. Suura, *Ann. Phys.* (NY) **13**, 379 (1961).
- [3] D. DeLaney, S. Jadach, Ch. Shio, G. Siopsis, B.F.L. Ward, *Phys. Rev.* **D47**, 853 (1993); *Phys. Lett.* **B292**, 413 (1992); *Phys. Lett.* **B302**, 540 (1993).
- [4] S.L. Glashow, *Nucl. Phys.* **22**, 579 (1961); S. Weinberg, *Phys. Rev. Lett.* **19**, 1264 (1967); A. Salam, in: *Elementary Particle Theory*, ed. N. Svartholm, Almqvist, Forlag AB, Stockholm 1968, p. 367; D.J. Gross, F. Wilczek, *Phys. Rev. Lett.* **30**, 343 (1973); H.D. Politzer, *Phys. Rev. Lett.* **30**, 1346 (1973); G. 't Hooft, unpublished.
- [5] S. Jadach, B.F.L. Ward, *Comp. Phys. Commun.* **56**, 351 (1990).
- [6] S. Jadach, B.F.L. Ward, *Phys. Rev.* **D40**, 3582 (1989).
- [7] S. Jadach, E. R.-Was, B.F.L. Ward, *Comp. Phys. Commun.* **70**, 305 (1992); *Phys. Lett.* **B268**, 253 (1991).
- [8] J. Rander, talk presented at CERN, May 1993; D. Miller, private communication, 1993; F. Merritt, APS Spring Meeting, 1993.
- [9] S. Jadach, MPI preprint, 1986.
- [10] S. Jadach, B.F.L. Ward, Z. Was, *Comp. Phys. Commun.* **66**, 276 (1991).
- [11] A. Akhundov *et al.*, *Nucl. Phys.* **276**, 1 (1986); D. Bardin *et al.*, *Z. Phys.* **C44**, 493 (1989).
- [12] W. Hollik, *Fortch. f. Physik* **38**, 65 (1990).
- [13] S. Jadach, Z. Was, R. Decker, J.H. Kuhn, *Comp. Phys. Commun.* **76**, 361 (1993).
- [14] See for example G. Altarelli, R. Barbieri, S. Jadach, *Nucl. Phys.* **B369**, 3 (1992); *Nucl. Phys.* **B376**, 444 (1992).
- [15] S. Jadach, B.F.L. Ward, *Phys. Lett.* **B274**, 470 (1992).
- [16] O. Adriani *et al.*, *Phys. Lett.* **B295**, 337 (1992).
- [17] G. Coignet, Proc. 1993 Lepton-Photon Conf., in press.
- [18] S. Jadach, B.F.L. Ward, S. Yost, to appear.

- [19] P.D. Acton *et al.*, CERN-PPE-92-215, 1992; G. Alexander *et al.* *Phys. Lett.* **B264**, 219 (1991); P. Abreu *et al.*, *Z. Phys.* **C53**, 555 (1992).
- [20] W. Beenakker, B. Pietrzyk, *Phys. Lett.* **B296**, 241 (1992).
- [21] See for example: L. Rolandi, Proc. 1992 Rochester Conf., ed. J. Sanford, AIP, New York 1992.
- [22] See for example: J. Rander, F. Merritt in Ref. [8].
- [23] S. Jadach, B.F.L. Ward, to appear.
- [24] S. Jadach, B.F.L. Ward, S.A. Yost, *Phys. Rev.* **D47**, 2682 (1993).
- [25] S. Jadach, M. Skrzypek, B.F.L. Ward, *Phys. Rev.* **D47**, 3733 (1993); UTHEP-93-0301, 1993.
- [26] S. Jadach, B.F.L. Ward, to appear.
- [27] S. Jadach, M. Melles, B.F.L. Ward, S.A. Yost, to appear.
- [28] F.A. Berends *et al.*, *Nucl. Phys.* **B297**, 429 (1988).
- [29] V.S. Fadin *et al.*, JINR-E2-92-577, Dec. 1992.
- [30] G. Faldt, P. Osland, BERGEN-1993-05, May 1993 and references therein.
- [31] G.P. Lepage, S.J. Brodsky, *Phys. Rev.* **D22**, 2157 (1980).
- [32] D. DeLaney *et al.*, to appear,
- [33] D. DeLaney *et al.*, UTHEP-93-0401, 1993.
- [34] B.F.L. Ward, *Phys. Rev.* **D36**, 939 (1987).
- [35] B.F.L. Ward, *Phys. Rev.* **D42**, 3249 (1990).
- [36] There are a number of related partial results in the literature. See, *e.g.*, J.M. Cornwall, G. Tiktopoulos, *Phys. Rev. Lett.* **35**, 338 (1975); *Phys. Rev.* **D13**, 3370 (1976); *Phys. Rev.* **D15**, 2937 (1977); J.M. Carrazzone, E.C. Poggio, H.R. Quinn, *Phys. Rev.* **D11**, 2286 (1975); *Phys. Rev.* **D12**, 3368 (1975); D.R. Butler, C.A. Nelson, *Phys. Rev.* **D18**, 1196 (1978); C.A. Nelson, *Nucl. Phys.* **B223**, 366 (1983); C.E.I. Canevio, J. Frenkel, J.C. Taylor, *Nucl. Phys.* **B269**, 235 (1986) and references therein.
- [37] F.A. Berends, W.T. Giele, *Nucl. Phys.* **B313**, 595 (1989).
- [38] See for example: R.K. Ellis *et al.*, *Nucl. Phys.* **B173**, 397 (1980); R.K. Ellis, J. Sexton, *Nucl. Phys.* **B269**, 445 (1986); D.B. DeLaney *et al.*, Ref. [32] and references therein.
- [39] See for example: F.A. Berends *et al.*, *Phys. Lett.* **B103**, 124 (1981); R.K. Ellis *et al.*, *Nucl. Phys.* **B173**, 397 (1980); R.K. Ellis, J. Sexton, *Nucl. Phys.* **B269**, 445 (1986).
- [40] See, *e.g.*, S. Weinberg, *Phys. Rev.* **D8**, 3497 (1973).